



GaInNAs/GaAs Bragg-mirror-based structures for novel 1.3 μm device applications

S. Calvez^{a,*}, J.-M. Hopkins^a, S.A. Smith^a, A.H. Clark^a, R. Macaluso^a, H.D. Sun^a, M.D. Dawson^a, T. Jouhti^b, M. Pessa^b, K. Gundogdu^c, K.C. Hall^c, T.F. Boggess^c

^a *Institute of Photonics, University of Strathclyde, Wolfson Centre, 106 Rottenrow, Glasgow G4 0NW, UK*

^b *Optoelectronics Research Centre, Tampere University of Technology, P.O. Box 692, FIN-33101, Tampere, Finland*

^c *Optical Science and Technology Center, Department of Physics and Astronomy, The University of Iowa, Iowa City, IA 52242, USA*

Abstract

We report the use of GaInNAs/GaAs material system for a range of 1.3 μm vertical-cavity devices namely VCSELs, VCISOAs, VECSELs and SESAMs. Using optical pumping, we demonstrate that up to 4 mW of 1290 nm output power can be fibre-coupled from a VCSEL. We also show that tailoring the VCSEL structure allows to produce a monolithic long-wavelength VCISOA with up to 16 dB of gain. We also report the first demonstration of a 1.3 μm VECSEL with more than 0.5 W of CW output power. Finally, annealing effects on the properties of a GaInNAs SBR and modelocking of two Nd:doped solid state lasers using this element are described.

© 2004 Elsevier B.V. All rights reserved.

Keywords: B1. Dilute nitrides; B2. Semiconducting III–V materials; B2. Semiconducting quaternary alloys; B3. Solid state lasers; B3. Vertical-cavity devices; B3. Vertical-cavity surface emitting lasers

1. Introduction

The GaInNAs/GaAs III–V–N semiconductor alloy system, first proposed by Kondow et al. in 1995/96 [1] has received considerable attention due to its suitability for developing advanced 1.3–1.5 μm laser diodes. As is now well-recognised, this alloy offers advantages including growth compatibility with AlGaAs-based distributed Bragg reflectors (DBRs), compatibility with wet thermal

oxidation processing techniques, reduced sensitivity to temperature, and economic benefits from being GaAs-substrate-based. The development of long-wavelength electrically driven vertical-cavity surface-emitting lasers (VCSELs) has been the primary driver of this research, and devices with very high specifications have been obtained and are on the route to commercialisation [2–4].

Because of this strong focus, the extension of the applications of GaInNAs structures to other important categories of 1.3 μm surface-normal devices has received little attention [5,6]. In this paper, we summarise our most recent progress in this area, more specifically our study of

*Corresponding author. Tel.: +44-141-553-4120; fax: +44-141-552-1575.

E-mail address: s.calvez@strath.ac.uk (S. Calvez).

diode-pumped high-power VCSELs, vertical *external-cavity* surface-emitting lasers (VECSELs), diode-pumped vertical-cavity semiconductor optical amplifiers (VCSOAs), and semiconductor saturable absorber mirrors (SESAMs) for laser mode-locking.

2. VCSELs/VCSOAs

2.1. Structures

The device structure utilised for VCSEL and VCSOA studies was originally designed for high-power laser operation under optical pumping, following the formalism developed in Refs. [7,8]. It consists of a 5λ active region surrounded by a 19-pair AlAs/GaAs top DBR and a 20.5-pair AlAs/GaAs bottom DBR. The active region contains six 6.7-nm thick $\text{Ga}_{0.64}\text{In}_{0.36}\text{N}_{0.014}\text{As}_{0.986}$ /GaAs quantum wells grown at 460°C and distributed over five anti-nodes of the standing wave pattern (two in the central fringe). The growth of this and the other structures reported here was carried out by molecular beam epitaxy (MBE) with a radio-frequency nitrogen plasma source; all structures except the SESAM (Section 4) were in situ annealed. All epitaxial layers were kept undoped as the VCSEL was designed specifically for optical pumping.

The room temperature reflectivity spectrum is presented in Fig. 1 together with the as-designed reflectivity curve. One can note that, because the

cavity is (deliberately designed) relatively long, two resonances appear within the stop-band of the device. Lasing only occurred at the long wavelength resonance because of gain alignment as indicated by the room temperature photoluminescence in Fig. 1. Recording these static characteristics across the 2-inch wafer (centre to edge) showed a spectral shift of the long wavelength resonance of below 15 nm indicating good lateral uniformity of the growth process.

For the VCSOA work, we etched back two pairs of the top mirror layers beforehand using reactive ion etching to increase the laser threshold value to obtain decent gain figures. The etching was monitored using an end-point detection system to appropriately stop at the interface.

In both cases, the structure was mounted on a temperature controlled copper mount using silver paint.

2.2. Set-up

The samples were studied under CW optical pumping using a wholly fibre-constituted system (see Ref. [9]) which included a commercially available 980 nm optically-pumped semiconductor laser (OPSL) as pump. An isolator (-35 dB of isolation) was inserted to avoid the formation an external cavity between the VCSEL and the OPSL pump laser. A $6.9\ \mu\text{m}$ -core 980 nm/1300 nm WDM coupler, whose common port was used to excite the VCSEL and couple out the 1300 nm laser emission. This common port was connected to a patchcord using an APC connector (referred as point A) while the other end of the patchcord was butt-coupled to the device. With this arrangement, up to 287 mW of 980 nm pump power reached the sample.

When studying laser performance, the laser emission was split in two after the WDM coupler to allow simultaneous power and spectral recording using computer-controlled and calibrated equipment. To allow direct comparison with other (electrically driven or optically pumped) reported devices, all presented results show the power at point A.

When investigating amplification, the signal was fed in and extracted using a circulator as

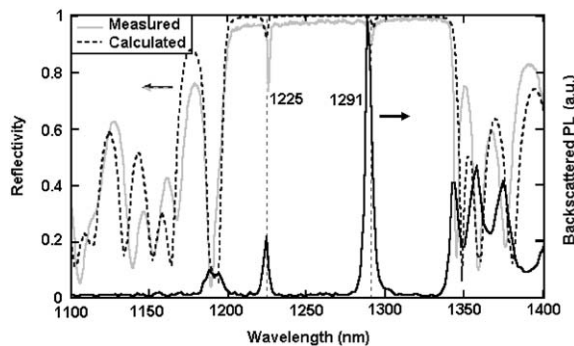


Fig. 1. Reflectivity and photoluminescence of the VCSEL sample at room temperature.

represented. The 1300 nm input signal was generated either by a tuneable laser (of wavelength resolution better than 0.005 nm) or by a superluminescent diode (SLD). Both were part of industry-standard, calibrated test units, the latter being integrated into the optical spectrum analyser which served as a diagnostic tool. The losses incurred in going from the input port of the circulator to the APC connection of the patchcord (point A) and from the APC connection of the patchcord to output port of the circulator were measured to be 2.8 and 2.3 dB, respectively. Knowledge of these losses allowed the extraction of fibre-to-fibre gain values which are independent of the testing arrangement and which can be compared directly to values in the literature.

2.3. Results

2.3.1. VCSEL

Optically pumped VCSELs have been investigated as a solution to reach long-wavelength emission because this injection scheme has two main advantages. First, as the structure is undoped, growth and processing are simplified and absorption loss is minimised. Second, longer mode-matched cavities can be used and tailored to achieve higher power output [7,10], improved dynamics [11] or add some functionalities like wavelength control [12].

We have worked to advance optically pumped GaInNAs VCSELs (Refs. [8,13–15]), and preliminary high-power data for a 15-well sample has been given [14,15]. Here, we report in full detail on the pertinent characteristics of a custom-designed high-power GaInNAs VCSEL structure with six quantum wells. The device assessment started by recording the VCSEL power transfer characteristic at 10°C. As can be seen in Fig. 2, threshold was reached for 217 mW of incident pump power, and the maximum obtained output power was 4.0 mW. The initial slope efficiency ($P_p < 260$ mW) is 8.4%. Assuming that the reflectivity for the top mirror is $R_{top} = 99.5\%$, that for the bottom mirror is $R_{bottom} = 99.6\%$, and neglecting intracavity absorption ($\alpha = 0$), the use of the formula given hereafter indicates a pump absorption efficiency of 19.8% for the in-well pumping

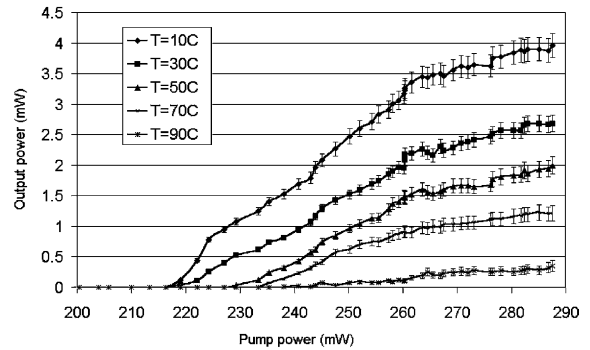


Fig. 2. Power transfer characteristics for several temperatures.

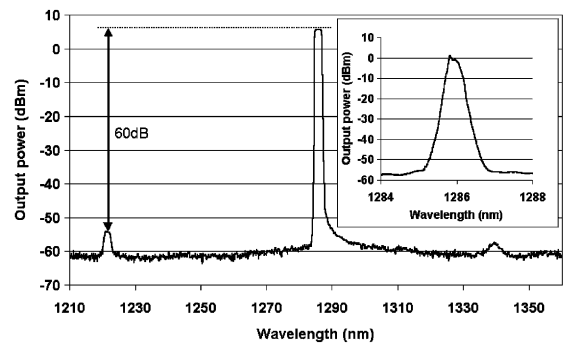


Fig. 3. Spectral characteristics of the laser emission at 10°C and under 287 mW of pump power.

scheme used here [8]:

$$\eta_{abs} = \eta \frac{\lambda_s \ln(R_{top} R_{bottom}) + \alpha L}{\ln(R_{top})}$$

Spectrally, the emission occurred at a wavelength of 1286.1 nm with a linewidth lower than the resolution of the OSA (0.06 nm) and a side-mode suppression ratio better than 60 dB (see Fig. 3).

We then investigated the performance of the device as the temperature of the mount was changed. Recording the spectra at maximum pump power for different sample temperatures in the range of 10–100°C, allowed us to observe a linear shift of ~ 0.11 nm/K (see Fig. 4) consistent with the induced change in the indices of refraction and thickness of the layers. The dependence of the maximum output power over the same temperature range is found to decrease almost linearly.

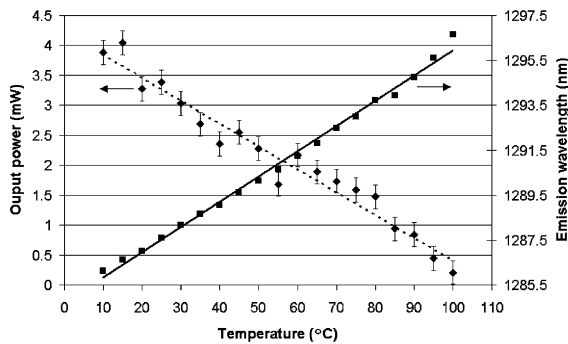


Fig. 4. Evolution of the maximum output power and wavelength of emission with temperature.

This decrease in the maximum output power is mainly associated with the decrease in slope efficiency (falling from 8.4% at 10°C to less than 0.4% at 90°C, as shown in Fig. 2). Several mechanisms could contribute to this phenomenon, for example, a less efficient in-well absorption of the pump (the overall reflectivity of the structure at the pump wavelength increases from 20% at 10°C to 45% at 90°C), an increase in the Auger recombination [16], or hole leakage [17].

2.3.2. VCSEA

Recently, Considerable attention has been devoted to the development of VCSEAs, for applications including optical interconnects, optical switching and wavelength-selective pre-amplifiers. This geometry of semiconductor optical amplifier offers advantages common to VCSEL technology, to which it is closely related, including high coupling efficiency to optical fibre, low-noise figure, polarisation insensitivity, and the facility for producing high-density, two-dimensional arrays

Until recently, demonstrations of 1.3 μm VCSEAs relied on wafer fusion technology, to produce hybrid structures with GaAs-based distributed Bragg reflectors (DBRs) and InGaAsP/InP multi-quantum well active regions [18–20]. In January 2003, we have reported initial results on GaInNAs VCSEA operation [21], which to our knowledge are the first monolithic VCSEA structures for 1.3 μm . This was undertaken with a sample which had had one pair of the top mirror etched off, and showed that 12.8 dB gain with

12 GHz bandwidth and saturation output power of -4.8 dBm were achievable using GaInNAs technology. Here, we further our investigations by studying the influence of temperature on the performance of a sample with 2-pair etched off from the top mirror.

Using an optical spectrum analyser, fibre-to-fibre gain spectra of the VCSEA were recorded for a number of different pump powers and temperatures. As the major changes in the device response occur at the cavity resonance (which varies with pump power and/or temperature), Fig. 5 shows the gain at resonance as a function of pump power. Except at 100°C, the gain versus pump power curves all share the same behaviour, indicating that the device performance is limited to on-chip gain lower than the threshold gain of 16 dB. At 100°C, however, the gain saturates to a value of 3 dB and threshold is never reached. Optimum performance is achieved when the device is the most efficient, i.e. around 55°C.

To gain a better understanding of how temperature affects the VCSEA performance, we monitored the pump power needed to achieve a given set of on-chip gain values. As represented in Fig. 6, all these curves follow the same trend. For temperatures between 40°C and 95°C, the pump power needed to reach a given gain value is nearly constant. The increase in the amount of pump power required to maintain a constant gain outside this window, is attributed to a larger offset between the wavelength at peak of the quantum-well gain and the cavity resonance and to an increase of non-radiative Auger recombinations at

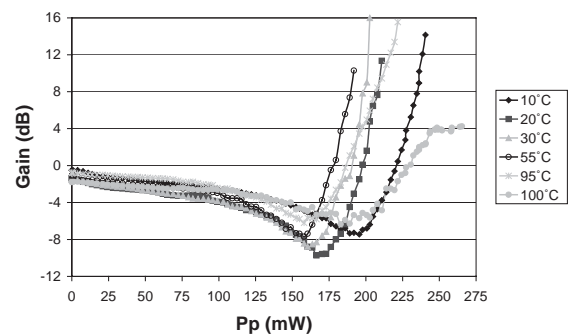


Fig. 5. Evolution of the VCSEA gain at resonance with pump power at different temperatures.

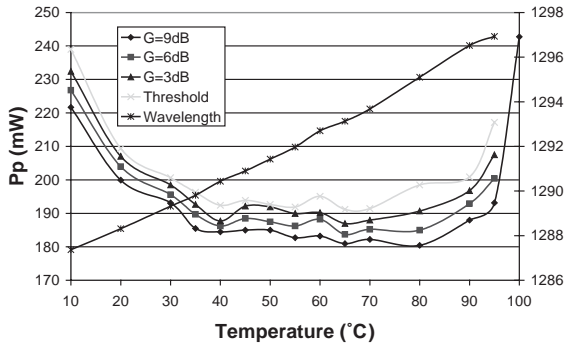


Fig. 6. Temperature dependence of the pump power requirement to reach different gain values and of the emission wavelength at threshold.

high temperatures. In addition to pump requirements, we also recorded the change in the emission wavelength at threshold. As can be seen in Fig. 6, a linear variation with temperature with a rate of 0.11 nm/K has been measured with no influence coming from the change in threshold pump power. This means that if the pump power can be sufficiently varied, our device can be operated with 9 dB of on-chip gain over a tuning range of 9.5 nm.

3. VECSELS

VECSELS relies on the use a half-cavity VCSEL with a free-space external cavity containing bulk optical elements and are a very attractive new format of semiconductor laser for telecommunications, but also for scientific, instrumentation and non-linear optics applications. Indeed, they offer, when appropriately mode-matched and designed, watt-level output in circularly symmetric diffraction-limited, TEM₀₀, output beams [22–24], and ready application of intracavity spectral and temporal control techniques for narrow-linewidth [25] or ultrashort pulse operation [26,27]. So far, VECSELS have mainly been developed around 1 μm and the use of GaInNAs/GaAs offers the opportunity to extend the wavelength coverage of this technology. Here, we present what we believe is the first demonstration of CW high-power 1.3 μm VECSEL operation using that material system.

The sample is constituted of a 25.5-pair GaAs/AlAs DBR on top of which has been grown a 4λ-cavity. The gain is provided by five sets of two Ga_{0.64}In_{0.36}N_{0.015}As_{0.985}/GaAs quantum wells positioned at the anti-nodes of the field and separated by 13 nm of barrier material (GaAs). The structure was grown under the same conditions as described for the VCSEL device and ex situ annealed for 1 s at 890°C. Static characterisation of the sample is shown in Fig. 7. Studying the PL temperature dependence under low-power excitation at 670 nm showed that the intensity peak reached a maximum at 80°C, suggesting that the optimum operation will be achieved when the active region temperature is around 80°C.

A 200 μm-thick diamond single crystal heat-spreader was bonded by the technique of liquid capillarity [28] to the surface of the semiconductor structure, and constitutes what the authors understand to be the first capillary bonding of diamond to a III–V epistructure. This composite element was then inserted in a copper mount with a regulated water cooling system and formed an end-mirror in a 3-mirror cavity as shown in Fig. 8. The HR curved mirror was located at ~54 mm from the substrate and the distance between the output coupler and the curved mirror was of ~72 cm ensuring both cavity stability and mode matching of the pump and signal beam in the gain region. The pump was a commercially-available 10 W fibre-coupled 810 nm diode array and up to 8.8 W was focused down to a ~75 μm diameter spot on the sample.

We started the characterisation by using a 1% output coupler and recorded the transfer

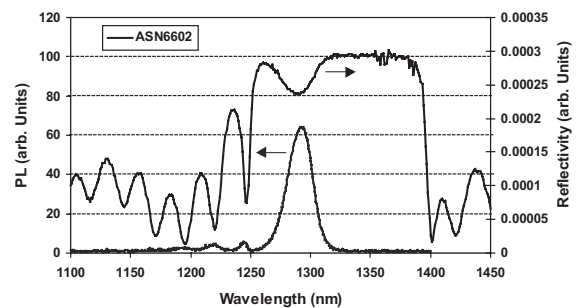


Fig. 7. Measured room temperature reflectivity and PL of the VECSEL sample.

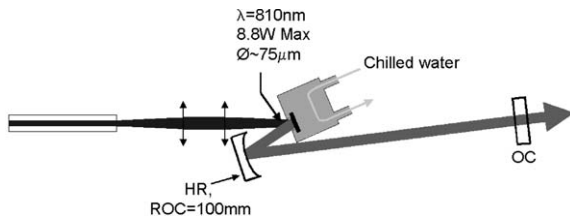


Fig. 8. VECSEL cavity arrangement.

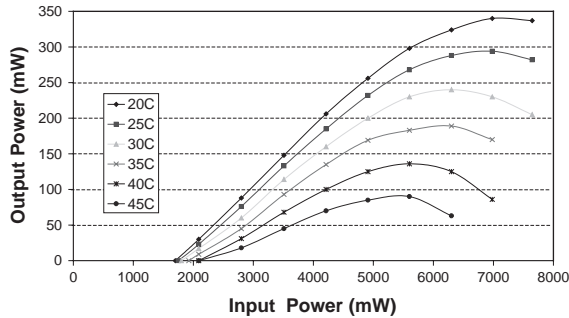


Fig. 9. Transfer characteristics of the VECSEL for different water temperature.

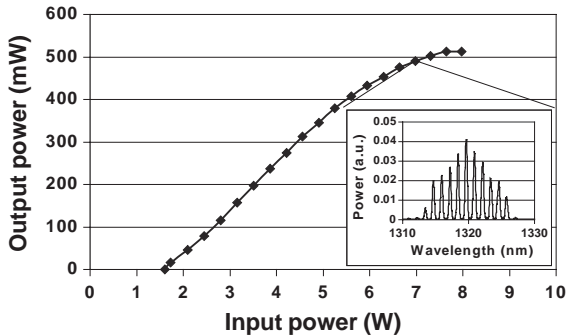


Fig. 10. Power transfer and spectral characteristic of the emission of the VECSEL with a 2% output coupler and 5°C water cooling.

characteristics for different water temperatures. As presented in Fig. 9, whichever temperature was used, it can be seen that all the curves share the same behaviour ending with a roll-over under high pump power injection. As the water temperature decreases, threshold decreases and higher output power can be achieved.

To obtain even higher powers, we kept the cavity identical but used a 2% output coupler, and cooled the device with water chilled to 5°C. Fig. 10 shows that threshold was obtained for an incident

pump power of 1.8 W and that the maximum output power reached 512 mW. The inset figure gives the spectral characteristics of the emission for 7 W of incident pump power. The spectrum was centred around 1319 nm and presented several peaks whose separation was related to the etalon formed by the bottom semiconductor mirror and the outer surface of the diamond.

4. SESAMs

The final family of GaInNAs surface-normal devices we have been investigating are SESAMs. These devices are passive modulator structures which have been shown to be very attractive for the self-starting and robust generation of ultrafast pulses from solid state— or more recently semiconductor— lasers. SESAMs in their optimal format have thus far been restricted to the wavelength range 800–1100 nm. As many semiconductor emitters and important DPSS lasers operate in the range 1.3–1.5 μm, a monolithically grown, low-loss SESAM for this spectral range is very desirable.

So far, the monolithic SESAMs designed for that wavelength range have not been ideal. Indeed, when made on GaAs, they used saturable regions which included either strain-relaxed InGaAs quantum-wells or a strain-relief buffer and showed significant residual non-saturable loss [29,30] while, when they were fabricated on InP, the limited refractive index contrast available within this material system restricted the high-reflectivity bandwidth.

The use of GaInNAs-on-GaAs is a way to overcome the latter issues as it not only allows single-step growth but does not require excessive strain. As a demonstration, a saturable Bragg reflector (SBR)-format SESAM, including a 21-pair AlAs/GaAs mirror centered at $\lambda = 1320$ nm and a single 7 nm-thick $\text{Ga}_{0.65}\text{In}_{0.35}\text{N}_{0.019}\text{As}_{0.981}$ quantum-well positioned in the middle of the top GaAs layer, was grown under conditions similar to those presented for the VCSEL but no in-situ annealing was performed to obtain a device as versatile as possible. The sample was annealed at $\sim 700^\circ\text{C}$ under nitrogen ambient, using a rapid

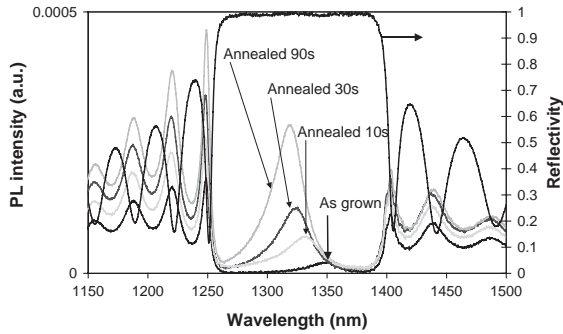


Fig. 11. Reflectivity and PL of the SESAM for as-grown and annealed samples (at 700°C for 10, 30 and 90 s).

thermal annealer for times up to 120 s. As shown in Fig. 11, as the annealing time increased, the PL peak emission blue-shifted by up to 30 nm and the PL intensity increased as a result of the alloy clustering minimisation and reduction of defect density. However, the reflectivity band of SBR hardly changed and the maximum reflectivity did not degrade.

Time-resolved PL measurements of both the as-grown and annealed (for 120 s) samples were performed using time-gated upconversion [31] at 300 K. With a modelocked (140 fs pulses, 76 MHz repetition rate) Ti:sapphire laser operating at $\lambda = 825$ nm with 6 mW of launched power focused down to a 60 μm -diameter spot and the excitation signal set so that the upconverted signal wavelength matches with the peak of the PL ($\lambda = 512.2$ and 505 nm, respectively), an increase of the decay time from ~ 69 ps (unannealed) to ~ 220 ps during the annealing process was recorded (see Fig. 12). Power dependence of the decay times has also been measured and the normalised decay time (with respect to the decay time obtained for 6 mW) is presented as the inset of Fig. 12. Similar increases in the decay time can be observed for both samples.

The latter two samples were used as low-loss ($<0.1\%$) passive-modelocking elements in Nd:YLF ($\lambda = 1314$ nm) and Nd:YALO ($\lambda = 1340$ nm) lasers. They allowed to demonstrate stable, high-average power generation of pulses with duration of ~ 24 ps from these two Nd:lasers and confirmed the effectiveness and tunable nature of the GaInNAs SBR [32]. Since then, the use of

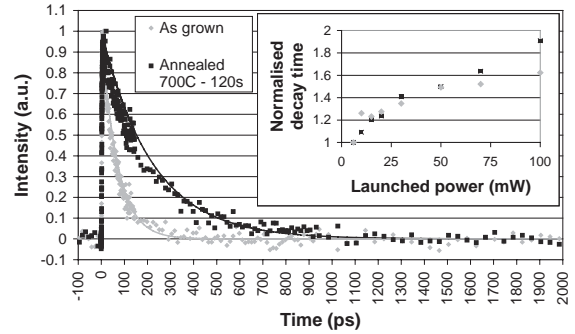


Fig. 12. Time-resolved PL measurements of the annealed (120 s) and as-grown SESAMs.

GaInNAs/GaAs SBRs has been extended to the 1.55 μm region where they have been used to modelock fibre lasers [33].

5. Conclusions

In this paper, we have demonstrated the ability to broaden the use GaInNAs/GaAs technology to other vertical-cavity devices than VCSELs. We have shown that this material system is particularly suited to demonstrate high-performance devices such as diode-pumped VCSELs with up to 4 mW of output power, diode-pumped VECSELs with output power greater than 0.5 W, diode-pumped vertical-cavity semiconductor optical amplifiers (VCSOs) with 9 dB of on-chip gain tunable over 9.5 nm, and the use of semiconductor saturable absorber mirrors (SESAMs) for high average power, picosecond Nd: laser mode-locking.

References

- [1] M. Kondow, K. Uomi, A. Niwa, T. Kitatani, S. Watahiki, Y. Yazawa, GaInNAs: a novel material for long-wavelength-range laser diodes with excellent high-temperature performance, *Jpn. J. Appl. Phys.* 1 35 (2B) (1996) 1273.
- [2] S. Sato, N. Nishiyama, T. Miyamoto, T. Takahashi, N. Jikutani, M. Arai, A. Matsutani, F. Koyama, K. Iga, Continuous wave operation of 1.26 μm GaInNAs/GaAs vertical-cavity surface-emitting lasers grown by metalorganic chemical vapour deposition, *Electron. Lett.* 36 (24) (2000) 2018.

- [3] L.M.F. Chirovsky, R.L. Naone, A.W. Jackson, S.R. Prakash, D. Galt, L. Thompson, S.A. Feld, J.G. Wasserbauer, M.J. Dalberth, J. Smith, J.J. Hindi, D.W. Kisker, 1.3 micron VCSEL arrays for telecom applications, Optical Fiber Communication (OFC) Conference 2002, Postdeadline paper, p. 149.
- [4] H. Riechert, L. Geelhaar, G. Ebbinghaus, A. Lima, A. Ramakrishnan, G. Steinle, "1.3 μm VCSELs for fiber-optical communication systems", Indium Phosphide and Related Materials (IPRM) 2003, Paper PLE2.
- [5] J.B. Heroux, X. Yang, W.I. Wang, GaInNAs resonant-cavity-enhanced photodetector operating at 1.3 μm , Appl. Phys. Lett. 75 (18) (1999) 2716.
- [6] Y.S. Jalili, P.N. Stavrinou, J.S. Roberts, G. Parry, Electro-absorption and electro-refract in InGaAsN quantum well structures, Electron. Lett 38 (8) (2002) 343.
- [7] M. Kuznetsov, F. Hakimi, R. Sprague, A. Moorelian, Design and characteristics of high power ($>0.5\text{CW}$) diode-pumped vertical-external-cavity surface emitting semiconductor lasers with circular TEM_{00} beams, IEEE J Select. Topics Quantum Electron. 5 (3) (1997) 561.
- [8] S. Calvez, D. Burns, M.D. Dawson, Optimisation of optically pumped 1.3 μm GaInNAs vertical-cavity surface-emitting lasers, IEEE Photon. Technol. Lett. 14 (2) (2002) 131.
- [9] S. Calvez, A.H. Clark, J.-M. Hopkins, R. Macaluso, P. Merlin, H.D. Sun, M.D. Dawson, T. Jouhti, M. Pessa, 1.3 μm GaInNAs monolithic vertical-cavity semiconductor optical amplifier, Indium Phosphide and Related Materials IPRM 2003, Paper WB1.3, (2003), pp. 243–246.
- [10] V. Jamarayan, T.J. Goodnough, T.L. Beam, F.M. Ahedo, R.A. Maurice, Continuous-wave operation of single-transverse-mode 1310-nm VCSELs up to 115°C, IEEE Photon. Technol. Lett. 12 (12) (2000) 1595.
- [11] C. Ellmers, F. Hohnsdorf, J. Koch, C. Agert, S. Leu, D. Karaiskaj, M. Hofmann, W. Stolz, W.W. Ruhle, Ultrafast (GaIn)(NAs)/GaAs vertical-cavity surface-emitting laser for the 1.3 μm wavelength regime, Appl. Phys. Lett. 74 (16) (1999) 2271.
- [12] D. Vakhshoori, P. Tayebati, C.-C. Lu, M. Azimi, P. Wang, J.-H. Zhou, E. Canoglu, 2mWCW singlemode operation of a tunable 1550 nm vertical cavity surface emitting laser with 50 nm tuning range, Electron. Lett. 35 (11) (1999) 900.
- [13] S. Calvez, A.H. Clark, J.-M. Hopkins, P. Merlin, H. Sun, M.D. Dawson, T. Jouhti, M. Pessa "Amplification, laser action in diode-pumped 1.3- μm GaInNAs vertical-cavity structures, IEEE Laser Electro-Optical Society Annual Meeting 2002, 1 Paper TuC4, (2002), pp. 165–166.
- [14] T. Jouhti, C.S. Peng, E.-M. Pavelescu, J. Konttinen, L.A. Gomes, O.G. Okhotnikov, M. Pessa, Strain compensated GaInNAs structures for 1.3- μm lasers, IEEE J. Select. Topics Quantum Electron. 8 (4) (2002) 787.
- [15] M. Pessa, C.S. Peng, T. Jouhti, E.-M. Pavelescu, W. Li, S. Karirinne, H. Liu, O.G. Okhotnikov, Towards high performance nitride lasers at 1.3 μm and beyond, IEE Proc. Optoelectron. 150 (1) (2003) 12–21.
- [16] S.R. Jin, S.J. Sweeney, S. Tomic, A.R. Adams, H. Riechert, Unusual increase of Auger recombination current in 1.3 μm GaInNAs-quantum-well lasers under high pressure, Appl. Phys. Lett. 82 (14) (2003) 2335.
- [17] N. Tansu, L.J. Mawst, The role of hole leakage in 1300-nm InGaAsN quantum-well lasers, Appl. Phys. Lett. 82 (10) (2003) 1500.
- [18] A. Karim, S. Bjorlin, J. Piprek, J.E. Bowers, Long-wavelength vertical-cavity lasers and amplifiers, IEEE J. Select. Topics Quantum Electron. 6 (6) (2000) 1244.
- [19] E.S. Bjorlin, B. Riou, P. Abraham, Y.-J. Chiu, J. Piprek, J.E. Bowers, 1.3 μm vertical cavity amplifier, IEEE Photon. Technol. Lett. 12 (8) (2000) 951.
- [20] E.S. Bjorlin, P. Abraham, D. Pasquariello, J. Piprek, Y.-J. Chiu, J.E. Bowers, High gain, high efficiency vertical-cavity semiconductor optical amplifiers, Indium Phosphide and Related Materials Conference - IPRM, (2002), pp. 307–310.
- [21] S. Calvez, A.H. Clark, J.-M. Hopkins, R. Macaluso, P. Merlin, H.D. Sun, M.D. Dawson, T. Jouhti, M. Pessa, 1.3 μm GaInNAs optically pumped vertical cavity semiconductor optical amplifier (VCSOA), Electron. Lett. 39 (1) (2003) 100.
- [22] S. Lutgen, T. Albrecht, P. Brick, W. Reill, J. Luft, W. Spath, 8-W high-efficiency continuous-wave semiconductor disk laser at 1000 nm, Appl. Phys. Lett. 82 (21) (2003) 3620.
- [23] W.J. Alford, T.D. Raymond, A.A. Allerman, High power and good beam quality at 980 nm from a vertical external-cavity surface-emitting-laser, J. Opt. Soc. Amer. B 19 (4) (2002) 663.
- [24] J.E. Hastie, J.-M. Hopkins, S. Calvez, C.W. Jeon, D. Burns, R. Abram, E. Riis, A.I. Ferguson, M.D. Dawson, 0.5-W Single transverse-mode operation of an 850 nm diode-pumped surface-emitting semiconductor laser, IEEE Photon. Technol. Lett. 15 (7) (2003) 894.
- [25] M.A. Holm, D. Burns, A.I. Ferguson, M.D. Dawson, Actively stabilized single frequency vertical-external-cavity AlGaAs laser, IEEE Photon. Tech. Lett. 11 (12) (1999) 1555.
- [26] S. Hoogland, S. Dhanjal, A.C. Tropper, J.S. Roberts, R. Haring, R. Paschotta, F. Morier-Genoud, U. Keller, Passively mode-locked diode-pumped surface-emitting semiconductor laser, IEEE Photon. Tech. Lett. 12 (9) (2000) 1135.
- [27] R. Haring, R. Paschotta, A. Aschwanden, E. Gini, F. Morier-Genoud, U. Keller, High-power passively mode-locked semiconductor lasers, IEEE J. Quantum Electron. 38 (9) (2002) 1268.
- [28] Z.L. Liao, Semiconductor wafer bonding via liquid capillarity, Appl. Phys. Lett. 77 (5) (2000) 651.
- [29] P.T. Guerreiro, S. Ten, E. Slobodchikov, Y.M. Kim, J.C. Woo, N. Peyghambarian, Self-starting mode-locked Cr:forsterite laser with semiconductor saturable Bragg reflector, Optics Commun. 136 (1-2) (1997) 27.
- [30] Z. Zhang, K. Torizuka, T. Itatani, K. Kobayashi, T. Sugaya, T. Nakagawa, Self-starting mode-locked femtosecond forsterite laser with a semiconductor saturable-absorber mirror, Opt. Lett. 22 (23) (1997) 1006.

- [31] L. Zhang L, T.F. Boggess, D.G. Deppe, D.L. Huffaker, O.B. Shchekin, C. Cao, Dynamic response of 1.3- μm -wavelength InGaAs/GaAs quantum dots, *Appl. Phys. Lett.* 76 (10) (2000) 1222.
- [32] H.D. Sun, G.J. Valentine, R. Macaluso, S. Calvez, D. Burns, M.D. Dawson, Low-loss 13 μm GaInNAs saturable Bragg reflector for high-power picosecond neodymium lasers, *Opt. Lett.* 27 (23) (2003) 2124.
- [33] O.G. Okhotnikov, T. Jouhti, J. Konttinen, S. Karirinne, M. Pessa, 1.5- μm monolithic GaInNAs semiconductor saturable-absorber mode locking of an erbium fiber laser, *Opt. Lett.* 28 (5) (2003) 364.